

BIOENGINEERING FUNCTIONAL COPOLYMERS. XV. SYNTHESIS OF ORGANOBORON AMIDE-ESTER BRANCHED DERIVATIVES OF OLIGO(MALEIC ANHYDRIDE) AND THEIR INTERACTION WITH HeLa AND L929 FIBROBLAST CELLS

Gülten KAHRAMAN^a, Mustafa TÜRK^b, Zakir M. O. RZAYEV^{c1,*},
M. Elif UNSAL^d and Ernur SÖYLEMEZ^{c2}

^a *Turkish Atomic Energy Authority (TAEK), Sarayköy Nuclear Research & Training Center, 06983 Ankara, Turkey; e-mail: gulten.kahraman@taek.gov.tr*

^b *Kırıkkale University, Department of Biology, Faculty of Arts and Sciences, Yahsihan, 71450 Kirıkkale, Turkey; e-mail: mtrk.35@gmail.com*

^c *Institute of Science & Engineering, Division of Nanotechnology and Nanomedicine, Hacettepe University, Beytepe, 06800 Ankara, Turkey; e-mail: ¹ zmo@hacettepe.edu.tr, ² esoylemez@gmail.com*

^d *Middle East Technical University, R & D Training and Measure Center, 06531 Ankara, Turkey; e-mail: egungor@metu.edu.tr*

Received July 2, 2010

Accepted November 23, 2010

Published online July 18, 2011

Novel bioengineering functional organoboron oligomers were synthesized by (i) amidolysis of oligo(maleic anhydride) (OMA) with 2-aminoethylidiphenylborinate (2-AEPB), (ii) esterification of organoboron oligomer (OMA-B) with α -hydroxy- ω -methoxypoly(ethylene oxide) (PEO) as a compatibilizer and (iii) conjugation of organoboron PEO branches (OMA-B-PEO) with folic acid as a tagging agent. Structure and composition of the synthesized oligomers were characterized by FTIR-ART and ^1H (^{13}C) NMR spectroscopy, chemical and physical analysis methods. Interaction of functional oligomers and oligomer-FA complex (OMA-B-PEO-F) with HeLa and L929 fibroblast cells were investigated by using different biochemical methods such as cytotoxicity, statistical, apoptotic and necrotic cell indexes, double staining and caspase-3 immunostaining, light and fluorescence inverted microscope analyses. It was found that citotoxicity and apoptotic/necrotic effects of oligomers significantly depend on the structure and composition of studied oligomers, and increase the following raw: OMA << OMA-B < OMA-B-PEO < OMA-B-PEO-F. A folic acid complex (MA-PEG-B-F) at 400 $\mu\text{g ml}^{-1}$ (2.36 $\mu\text{mol ml}^{-1}$) concentration as a therapeutic drug exhibits minimal toxicity toward the fibroblast cells, but influential for HeLa cells.

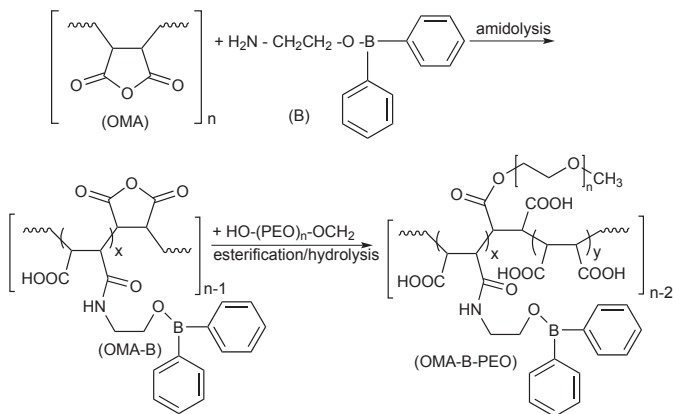
Keywords: Synthesis; Amidolysis; Organoboron oligomers; Conjugation; Cytotoxicity; Apoptotic and necrotic effects.

During much years in literature, the ruling opinion about non-polymerizability of maleic anhydride (MA) because of steric factor and sym-

metrical structure as a 1,2-substituted olefin was existed. However, many researchers radically refute this thesis and they demonstrated that MA can be polymerized by various methods, such radical solution¹⁻³, electrochemical⁴, plasma⁵, UV-^{1,6} and γ -irradiation^{1,7}, high pressure^{8,9} and solid state¹⁰ polymerizations, in the different chosen conditions with formation of low [oligo(MA)] or high molecular weight [poly(MA)] polymers. First Walker et al.⁹ reported about possibility of polymerization of MA under high pressure (3300–12000 atm, 20–125 °C) with formation of oligomer products. Poly(MA) and their derivatives has very good performance of scale inhibitor and dispersant, widely used in industrial cooling water, boiler water, oil field injection, sugar mill evaporator, reverse osmosis, desalination and bioengineering applications^{1-3,11,12}. Water-soluble compound derived from a homopolymer of MA having available anhydride functional groups and hydrolyzed anhydride functional groups (carboxylic groups) carrying a residue of a primary, secondary or tertiary amine functional group or the sulfur atom of a thiol functional group¹¹. However, synthesis and bioengineering investigations of the organoboron functionalized derivatives of oligo(MA) are not reported. On the other hand, organoboron compounds and organoboron functionalized polymers have been known for over a century, and many aspects of their chemical, biological, therapeutic and bioengineering properties have been known for quite some time¹³⁻¹⁷. These include certain boron analogues of biomolecules¹⁸, RNA- and glucose-sensitive organoboron polymers¹⁵, antibacterial and antimalarial agent diazaborine¹⁹, various antibacterial oxazaborolidines²⁰, the antibacterial di-phenyl borinic esters that inhibit bacterial cell wall growth²¹, the anti-fungal agent benzoxaborole²² and an estrogen receptor modulator containing a B-N bond²³. Boron-containing molecules, including boronic acids and carboranes, also investigated as agents for boron-neutron capture therapy (BCNT) for the treatment of brain tumours^{14,24,25}. Vazquez and Navarro²⁶ described recent approaches to be applied for the therapeutic management of patients with cancer. According to the authors, a multimodal approach of therapy including surgery, conventional chemotherapy and radiotherapy was applied with irregular success, making it the best known combination for survival at the early diagnostic stage, as well as having created a revolution in the field of oncology.

The goal of this work is synthesis and characterization of novel organoboron amide derivatives by amidolysis of oligo(MA) with 2-aminoethyl-diphenyl borinate (2-AEPB) and their α -hydroxy- ω -methoxy-poly(ethylene oxide) (PEO) macrobranches by grafting of synthesized organoboron oligomer with PEO to improve biocompatibility and degree of conjugation

with biomacromolecules. An important aspect of this work is comparative investigations of the interactions of these novel boron-containing oligomer systems with HeLa (human cervix carcinoma cell) and L 929 fibroblast cells, and evaluation of their antitumor activity (cytotoxicity, apoptotic and necrotic effects) using various biochemical methods such as hematoxylen/eosin and immuno cytochemical stainings, light and fluorescence inverted microscopy analyses. Synthetic pathways of the side-chain amide-ester-carboxylic functionalized organoboron oligomers can be represented as follows (Scheme 1).



SCHEME 1

Synthetic routes of the organoboron amide-ester-carboxylic oligomers (OMA-B and OMA-B-PEO)

EXPERIMENTAL

Materials

Maleic anhydride monomer (Fluka, Switzerland) was purified by recrystallization from anhydrous benzene solution and sublimation in vacuum. Benzoyl peroxide (BP) (Fluka) as a radical initiator was recrystallized twice from benzene before use. 2-Aminoethyl diphenylborinate (2-AEPB) (Sigma-Aldrich, Germany) was purified by recrystallization from anhydrous ethanol: m.p. 193.5 °C (by DSC). FTIR-ATR spectra of 2-AEPB (v, cm⁻¹): 3284 (vs) and 3220 (s) N-H stretching in NH₂, 3066 (vs)-2870 (s) C-H stretching, 1611 (vs) NH₂ bending and C=C stretching in phenyl groups, 1491 (m) and 1334 (m) B-O band, 1432 (vs) fairly strong, sharp band due to benzene ring vibration in phenyl-boronic acid linkage, 1263-1154 (s) fairly strong, sharp bands due to C-N stretching in C-NH₂, 1061 (vs) N-H bending in NH₂ and 750-710 (s) sharp bands due to boron-phenyl linkage. ¹H NMR spectra (δ, ppm) in CHCl₃-d₁: CH₂-O 1.49, CH₂-NH₂ 2.96, and 7.38-7.40 (1 H), 7.19-7.24 (2 H) and 7.13-7.16 (2 H) for protons of *p*-, *o*- and *m*-positions in benzene ring, respectively. α-Hydroxy-ω-methoxy-PEO (M_n 2000 g mol⁻¹) (Fluka): ¹H NMR spectra (δ, ppm) in

$\text{CHCl}_3\text{-}d_1$: $\text{CH}_2\text{-O}$ 3.75–3.45, OH end group 2.61 and O-CH_3 end group 2.16. *N*-Ethyl-*N*-(3-dimethylaminopropyl)carbodiimide hydrochloride (EDAC) as a catalyst and folic acid (FA) as a targeting agent were supported from Aldrich–Sigma (Germany). All solvents and reagents were of analytical grade and used without purification.

HeLa (human cervix carcinoma cell) cancer cells and L929 fibroblast cells were obtained from the tissue culture collection of the SAP Institute (Ankara, Turkey). Cell culture flasks and other plastic material were purchased from Corning (NY, USA). The growth medium, which is Dulbecco Modified Medium (DMEM) without L-glutamine supplemented fetal calf serum (FCS), and Trypsin-EDTA were purchased from Biological Industries (Kibbutz Beit Haemek, Israel). The primary antibody, caspase-3 was purchased from Lab Vision (Germany).

Synthesis of Oligo(maleic anhydride)

Heterogeneous solution homopolymerization of MA was carried out in toluene at 80 °C with BP initiator under the nitrogen atmosphere. Reaction conditions: $[\text{toluene}]/[\text{MA}] = 3$, $[\text{MA}] = 2.5 \text{ mol l}^{-1}$ and $[\text{BP}] = 0.026 \text{ mol l}^{-1}$. Appropriate quantities of MA monomer and BP were placed in a standard pyrex-glass reactor, and the reaction mixture was cooled by liquid nitrogen and flushed with dried nitrogen gas for at least 5 min, then sealed and placed in a thermostated silicon oil bath at 80 °C. During the reaction, the formed powder product with light-brown color began to precipitate after the first hour. At the end of reaction time, powder product was isolated from reaction medium by filtration. Then prepared product was dissolved in acetone and precipitated with benzene. This procedure was repeated twice. Then white powder product was dried at 40 °C under vacuum. Synthesized oligo(MA) has the following average parameters: $d = 1.24 \text{ g cm}^{-3}$, acid number 112.5 mg KOH/g (by alkali titration), the weight-average molecular weight (M_w) 7480 g mol⁻¹ (by DLS), glass-transition temperature (T_g) 81.1 °C (by DSC). Structure of MA oligomer was confirmed by FTIR and NMR spectroscopy. FTIR-ATR spectra (ν, cm^{-1}): 2970 (m) for backbone CH stretching band, 1842 (w), 1774 (m) and 1703 (s) bands for antisymmetrical and symmetrical C=O band of MA unit, 1226 (w-m) and 1173 (m, broad) anhydride C–O–C stretching. ¹H NMR spectra (δ, ppm) in $\text{DMSO-}d_6$ at 25 °C: 2 H around 2.5–4.0 for backbone CH-CH group in MA unit. ¹³C NMR (DEPT-135) spectra (δ, ppm): (1) 170 for anhydride C=O 170 and 45.0 CH backbone in CH-CH group.

Synthesis of 2-Amidoethylidiphenylborinate-oligo(maleic acid)

Amidolysis of oligo(MA) with 2-AEPB using various [MA unit]/[2-AEPB] mole ratios was carried out in *N,N'*-dimethylformamide (DMF) at 60 °C with EDAC catalyst under the nitrogen atmosphere using a standard pyrex-glass reactor supplied by a mixer, temperature control unit and condenser. Reaction conditions: [2-AEPB] = 0.066 mol l⁻¹, mole ratios of [MA unit]/[2-AEPB] = 1:1, 3:1, 5:1 and EDAC = 1.0 wt.%. Appropriate quantities of oligo(MA), 2-AEPB, DMF and EDAC were placed in a reactor and the reaction mixture was flushed with dried nitrogen gas for at least 2 min, then sealed and placed in a thermo stated silicon oil bath at 60 °C to intensive mixing for 5 h. The organoboron amide oligomer was isolated from reaction mixture by precipitation with diethyl ether and dried under vacuum. Synthesized organoboron oligomer has the following average parameters: M_w 7720 g mol⁻¹ (by DLS), T_g 155.8 °C (by DSC), $[\eta]_{in}$ 0.02 l g⁻¹ in deionized water at 25 °C. FTIR-ATR spectra (ν, cm^{-1}) of oligo(MA)-g-2-AEPB (KBr pellet): 1693 (m) C=O stretching (amide I band), 1649 (m) and 1564 (m) N–H deformation (amide II band), 1436 (w) and 1386 (m) C–N stretching

(amide III band). ^1H NMR spectra (δ , ppm) in $\text{DMSO}-d_6$ at 25 °C: protons of phenyl groups 6.9–7.18, 2 H from CH_2 in $-\text{CH}_2\text{-CO-NH-}$ fragment 5.8, 2 H from B-O-CH_2 group 3.4, 2 H from backbone $-\text{CH-CH-}$ 3.1, and 2 H from NH-CH_2 group 2.7. ^{13}C NMR spectra (δ , ppm): C=O of MA unit 177, C=O of amide linkage 173, CH= in phenyl groups 162–158, C-N 136 and 126, backbone CH 46, NH-CH_2 41–42, $\text{CH}_2\text{-O}$ 31–36.

Synthesis of 2-Amidoethyl Diphenylborinate-PEO-ester-oligo(maleic acid)

The esterification (grafting) of organoboron amide oligomer, containing 19.24 mole % of organoboron linkages and 80.76 mole % of free anhydride units, with PEO (M_n 2000 g mol $^{-1}$) at oligomer/PEO feed molar ratio 1:0.01 was carried out in DMF at 60 °C for 1 h. PEO branched oligomer was isolated from reaction mixture by precipitation with diethyl ether and dried 40 °C under vacuum. Prepared PEO ester of organoboron oligomer has the following average characteristics: M_w 8100 g mol $^{-1}$ (by DLS), T_g 129 °C (by DSC). ^1H NMR spectra (δ , ppm) in $\text{DMSO}-d_6$ at 25 °C: protons of phenyl groups 7.2, CH_2 in $\text{CH}_2\text{-CO-NH-}$ amide linkgae 6.0, weak and broad O-CH_2 in PEO branch 4.7, 2 H in B-O-CH_2 3.6, CH_2CH_2 in PEO branch 3.5, 3 H in OCH_3 end group 3.2, backbone CH 3.1, and 2 H in NH-CH_2 2.7. ^{13}C NMR spectra (δ , ppm): C=O of MA unit 176, C=O of amide group 173, 5 CH= in phenyl groups 162–158, C-N 136–126, CH_2CH_2 in PEO branch 71–72, O-CH_2 in PEO 69, (7) end OCH_3 group of PEO 58, backbone CH 46, NH-CH_2 41–42, and $\text{CH}_2\text{-O-B}$ 31–36.

Characterization

Fourier transform infrared (FTIR-ATR) spectra were recorded with FTIR Nicolet 8700 spectrometer in the 3700–600 cm $^{-1}$ range. ^1H and ^{13}C NMR spectra were performed on a Bruker Avance (300 MHz) spectrometer with $\text{DMSO}-d_6$ as a solvent at 25 °C.

Composition of organoboron oligomers was determined using the following equation

$$m_1 \text{ (B-MA-unit mole \%)} = \frac{100 M_2}{(A_B / B) - (M_2 - M_1)} \quad (1)$$

where B is boron content in organoboron oligomer (wt.%), A_B is atom weight of boron, M_1 and M_2 are molecular weights (g mol $^{-1}$) of organoboron (m_1) and non-grafted MA (m_2) units ($m_1 + m_2 = 100$ mole %).

Thermogravimetric (TGA) and differential scanning calorimetry (DSC) analyses were performed in a Thermal TGA-DTA Analyzer (Shimadzu DTG-60H, Japan) and Shimadzu DSC-60 Analyzer (Kyoto, Japan), respectively, under nitrogen atmosphere at a heating rate of 10 °C min $^{-1}$.

The weight-average molecular weight (\bar{M}_w) of the functional oligomers was determined by dynamic light scattering (DLS) method using a Malvern CGS-3 DLS Analyzer.

The intrinsic viscosities of the organoboron oligomers were determined in deionized water at 25 ± 0.1 °C in the concentration range 0.05–1.5 g dl $^{-1}$ using an Ubbelohde viscometer.

To determine the cytotoxicity, different amounts of OMA, OMA-B, OMA-PEO-B and OMA-PEO-B-F functional oligomers (about 0–6.63 $\mu\text{m ml}^{-1}$ in aqueous solutions) were placed in DMEM and then were put into 24-well plates containing HeLa and L 929 fibroblast cells (50×10^3 cells per well), respectively. HeLa cells were harvested with trypsin-EDTA, and then were stained with trypan blue dye. The number of living and dead

cells were counted with a haemacytometer (C.A. Hausse & Son Phluila, USA), using light microscope at $\times 200$ magnification²⁷. HeLa and fibroblast cells (20×10^3 cells per well) were also treated with different amount functional oligomers for 24 h, after removing the medium were stained with hematoxylen/eosin and then images of the cells were recorded by light inverted microscopy (Leica, Germany)²⁷.

Analysis of apoptotic and necrotic cells with double staining were performed to quantify the number of apoptotic cells in culture on basis of scoring of apoptotic cell nuclei. HeLa and L929 fibroblast cells (20×10^3 cells per well) in growth medium treated with different amount functional oligomers in aqueous solutions for 24 h period, both the attached and detached cells were collected, then stained with Hoechst dye 33342 ($2 \mu\text{g ml}^{-1}$), propodium iodide (PI) ($1 \mu\text{g ml}^{-1}$) and DNase free-RNAse ($100 \mu\text{g ml}^{-1}$) for 15 min at room temperature^{28,29}. Necrotic cells were staining red by PI. Necrotic cells lacking plasma membrane integrity and PI dye cross cell membrane, but PI dye does not cross non necrotic cell membrane. The numbers of apoptotic and necrotic cells were determined with DAPI and FITC filters of fluorescence inverted microscope (Leica, Germany).

To determine the Caspase-3 activity, a known method of apoptotic detection of HeLa cells with minor modification was utilized³⁰. In brief, for caspase-3 immunocytochemistry, collected HeLa cells were treated in 3% H_2O_2 for 5 min and rinsed with PBS for 15 min. The cells were blocked with blocking solution in PBS and then incubated (45 min, room temperature) with primer antibody caspase-3 (Lab Vision, 1:300 dilution) in PBS. The cells were then incubated with biotin-conjugated secondary antibody (1:300, 1 h, room temperature), avidin-biotin-peroxidase complex (Santa Cruz Biotechnology, Inc., rabbit peroxidase kit; 1 h) and DAB solution. Sections were counterstained with hematoxylin. For negative controls, primary antibody was omitted in one of the slides.

RESULTS AND DISCUSSION

Structure of Organoboron Oligomers

The structures of synthesized organoboron oligomers and their PEO branches were confirmed by FTIR-ATR and ^1H (^{13}C) NMR spectra, comparative analysis of FTIR-ATR spectra (Fig. 1) of 2-AEPB, oligo(MA) and its organoboron derivative indicates that the characteristic bands of anhydride C=O groups disappearance in the spectra of OMA-B-1 oligomer prepared from equimolar feed ratio of oligo(MA):2-AEPB. The formation of amide bound in this organoboron oligomer is confirmed by the appearance of new bands such as 1693 (amide I band), 1649 and 1564 (amide II band), 1436 and 1386 (amide III band). Simultaneously a very broad band between 3500 and 2800 cm^{-1} appears in spectra due to increase hydrogen bonded fragments in organoboron oligomer (OMA-B-1). The intensities of amide bands significantly decrease in spectra of OMA-B-2 and OMA-B-3 oligomers prepared from oligo(MA)/2-AEPB mixtures enchainig with OMA oligomer (OMA >> 2-AEPB).

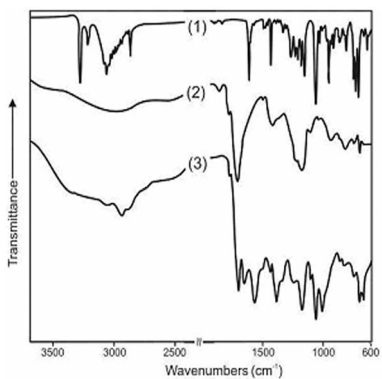


FIG. 1
FTIR spectra of 2-AEPB (1), oligo(MA) (2) and oligo(MA)-g-2-AEPB (3)

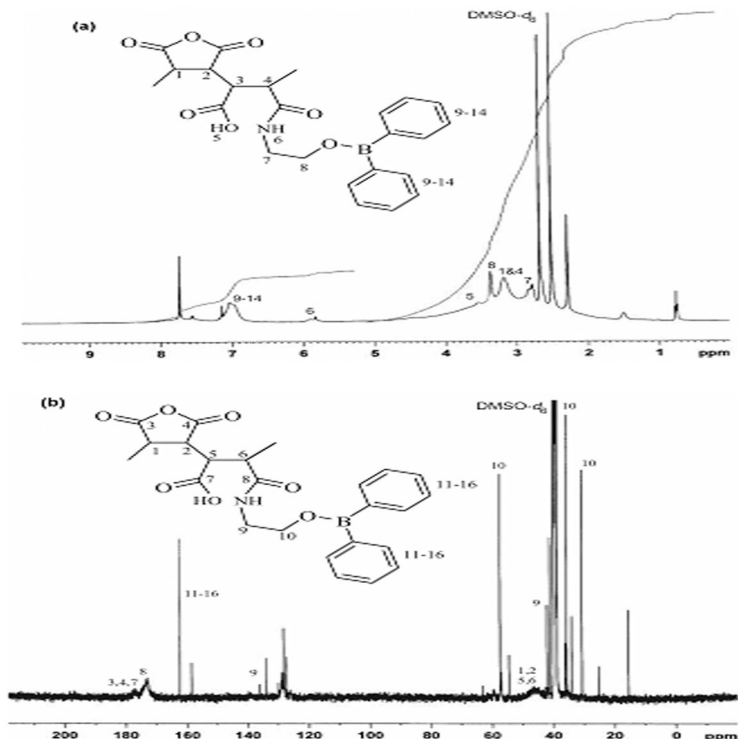


FIG. 2
 ^1H NMR (a) and ^{13}C NMR (b) spectra of oligo(MA)-g-2-AEPB in $\text{DMSO}-d_6$

Similar effect has been observed from comparative analysis of the ^1H and ^{13}C NMR spectra of OMA-B-2 and its PEO branch (OMA-B-PEO). The results of this analysis are illustrated in Figs 2 and 3. The formation of H-bonded amide linkages is confirmed by a presence of characteristic broad peaks at 5.8 and 173 ppm in the ^1H and ^{13}C NMR spectra of OMA-B-2, respectively (Fig. 2). In addition, the presence of characteristic proton peaks of organoboron linkages such as quarter phenyl peak at 6.9 ppm, triplet B-O-CH₂ peak at 3.4 ppm and quarter NH-CH₂ peak at 2.7 ppm (Fig. 2a) also confirmed that 2-AEPB is covalently bound to anhydride units. In the ^{13}C NMR spectra of OMA-B-2 oligomer (Fig. 2b), the characteristic carbon resonances (162, 158, 136, 126, 41, 42, 31 and 36 ppm) from organoboron fragment are also observed.

^1H (^{13}C) NMR spectra of PEO grafted organoboron oligomer (OMA-B-PEO) are illustrated in Fig. 3. The observed proton signals of side-chain PEO branches at 4.7, 3.5 and 3.2 ppm for (CH₂-CH₂-O)_n units (Fig. 3a) and car-

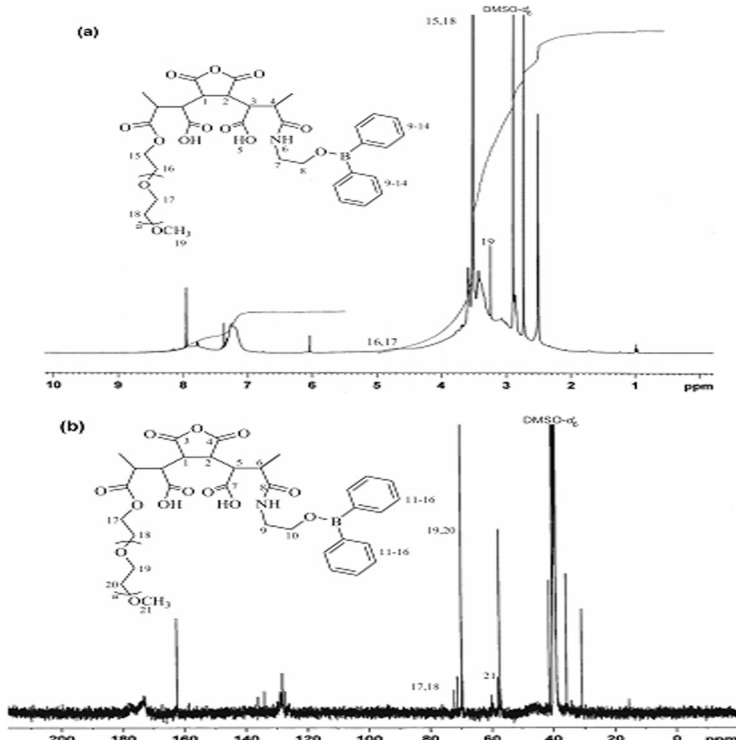


FIG. 3
 ^1H NMR (a) and ^{13}C NMR (b) spectra of oligo(MA-g-2-AEPB-g-PEO) in $\text{DMSO}-d_6$

bon atom resonances (71 and 72 ppm for CH_2CH_2 , 69 ppm for $\text{O}-\text{CH}_2$ and 58 ppm for OCH_3 end group) (Fig. 3b) can be regarded as an additional fact to confirm the formation of side-chain macrobranched PEO linkages.

Functional Oligomer Composition–Property Relations

The results of intrinsic viscosity measurements from η_{sp}/c (specific viscosity versus oligomer concentration in deionized water) plots for the OMA and its organoboron and PEO derivatives having different compositions are illustrated in Fig. 4. A visible decrease of η_{in} value with increasing the organoboron fragment in oligomer was observed (Table I). As seen from these data, unlike the pristine OMA and PEO branched derivative the organoorganoboron oligomers exhibit typical polyelectrolyte behavior, i.e. increase in viscosity with a dilution of oligomer water solution, which can be explained by specific behaviour of complexed macromolecules and their conformational changes resulting in the expansion of polymer coil in the dilution solution. Similar effect was observed for the other carboxyl-containing polymers such as poly(acrylic acid)³¹ and maleic acid copolymers^{32,33}.

Thermal behavior and phase transitions of synthesized oligomers were investigated by differential scanning calorimetry (DSC) and thermal gravimetric analysis (TGA) methods. The obtained results are summarized in Fig. 5. It was found that OMA and its organoboron and PEO branched derivatives exhibit amorphous structure with characteristic broad *endo*-

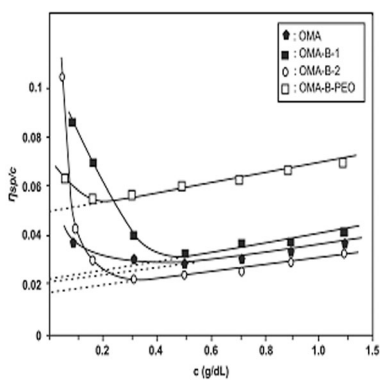


FIG. 4

The plots of η_{sp}/c (specific viscosity versus oligomer concentration in deionized water):
 ● OMA, ■ OMA-B-1, ○ OMA-B-2 and □ OMA-B-PEO

TABLE I
Some characteristic parameters of MA oligomer and its organoboron amide and PEO ester branched derivatives

Functional oligomers (from reaction mixture, mole ratio)	B %	$[\eta]_{\text{in}}, \text{dl g}^{-1}$ in water at 25 °C	T_g °C	M_w g mol ⁻¹	Oligomer composition, mole%			
					B-MA, m_1	MA, m_2	PEO	FA
Oligo(MA) (1:0)	0.0	0.021	95.2	7480	—	100	—	—
OMA-B-1 (1:1)	3.35	0.025	155.0	7720	21.19	78.81		
OMA-B-2 (3:1)	2.08	0.018	142.8	7600	15.96	84.04		
OMA-B-3 (5:1)	1.51	0.013	133.5	7530	12.58	87.42		
OMA-B-2-PEO (3.08:1:0.04)	1.86	0.055	128.6	8100	14.49	84.36	1.15	—
OMA-B-2-PEO-FA (2.96:1:0.04:0.02)	~1.86	—	—	—	14.26	83.97	1.18	0.59

peaks, which are associated with the glass-transition temperatures (T_g), significantly depend on the composition and content of organoboron linkages in the functional oligomers. The higher values of T_g are observed for the oligomers containing relatively high organoboron linkages. Therefore, rigid H-bonded structure provides high T_g in the organoboron oligomers (curves 1–3). For the pristine OMA (curve 5) and PEO branched derivative (curve 4) the relatively low values of T_g are observed.

The results of TGA analyses (Fig. 5) indicate that the organoboron and PEO branched derivatives of OMA show higher thermal stability which increases with increasing degree of grafted organoboron linkage in the oligomer. The observed two step degradation of the OMA and its functionalized derivatives indicates occurrence of some macromolecular reactions, specifically, anhydridization of free carboxylic groups, proceeding before decomposition of oligomers. TGA analyses also allow us to determine the content of boron in studied functionalized oligomers, and therefore, calculate their molar compositions, results of which are summarized in Table I.

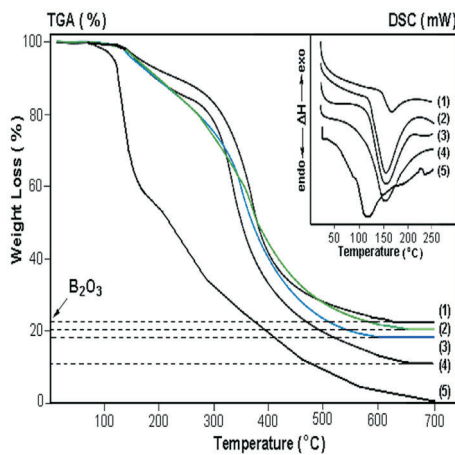


FIG. 5
DSC and TGA curves of the functional organoboron oligomers: OMA-B-1 (1), OMA-B-2 (2), OMA-B-3 (3), OMA-B-PEO (4) and pristine oligo(MA) (5). Heating rate $10\text{ }^{\circ}\text{C min}^{-1}$ under nitrogen atmosphere

Cytotoxicity

The obtained cytotoxicity results of the pristine oligo(MA) (OMA) and its organoboron amide (OMA-B) and organoboron amide-ester (OMA-B-PEO) branches, and OMA-B-PEO/folic acid complex (OMA-B-PEO-F) on cancer cells using a Trypan blue staining were illustrated in Fig. 6. As seen from plots of concentration of polymers versus per cent of cell viability, the toxicity of pristine OMA against HeLa and fibroblast cells decreased with increasing in polymer concentration from 0.51 to 6.63 $\mu\text{mole ml}^{-1}$ for 24 h incubation at 37 °C. If oligomer concentration was higher than 6.63 $\mu\text{mole ml}^{-1}$, its toxicity increased for 24 h incubation. The toxicity of OMA-B (organoboron amide oligomer) was more significant than other oligomer systems. Figure 6 shows that the number of viable cells is above 80% for fibroblast and HeLa cells after incubation of the cells with OMA-B at concentrations around 0.33–4.36 $\mu\text{mole ml}^{-1}$ for 24 h incubating time in cell culture media. The number of viable cells was over 50% for normal cells in the range of 2.68–4.36 $\mu\text{mole ml}^{-1}$ concentration. However, the toxicity for HeLa cells significantly increases for concentrations above 2.68 $\mu\text{mole ml}^{-1}$. OMA-B and OMA-B-PEO-F complex had higher toxicity for HeLa cells (35% alive cells) than fibroblast cells (48% alive cells) in 4.36 and 3.83 $\mu\text{mole ml}^{-1}$ concentrations, respectively. When PEO was added to the structure (OMA-B-PEO), the cytotoxicity was decreased because of PEO biocompatibilization effect. The cytotoxicity of PEO containing oligomer

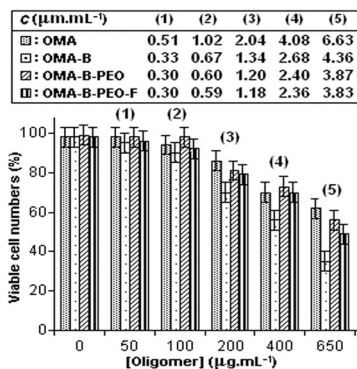
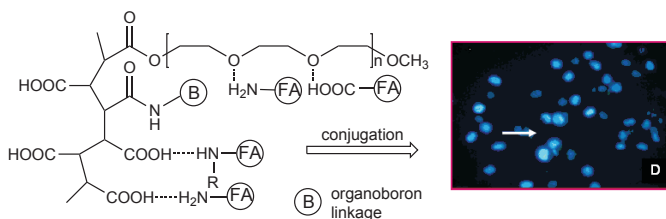


FIG. 6

In vitro cytotoxicity of OMA, OMA-B, OMA-B-PEO and OMA-B-2-PEO-F functionalized oligomers with different amount at 24 h incubation. Viable of HeLa cells in wells (in %). Results are presented as means \pm SEM

was lower than those without PEO at $2.4\text{--}3.87\text{ }\mu\text{mole ml}^{-1}$ concentration (Fig. 6). To improve the targeting of oligomer macromolecules to HeLa cells, folic acid (FA) was inserted to the structure through complex-formation. The formation of oligomer...FA complex through interaction amine groups of FA with ester groups of branched PEO and free carboxylic groups and its conjugation with HeLa cells may be schematically



SCHEME 2

Proposed structure of organoboron oligomer...FA (folic acid) conjugate with cancer cells

represented as follows (Scheme 2).

The toxicity of the oligomer...FA complex for the cancer cells is significantly higher than that for the normal cells as cancer cells have higher number of FA receptors than normal cells.

Hematoxylen/Eosin Staining Results

For the morphological observations in the oligomer-cell systems, the mixtures of the pristine OMA ($0.6\text{--}6.63\text{ }\mu\text{mole ml}^{-1}$), OMA-B ($0.33\text{--}4.36\text{ }\mu\text{mole ml}^{-1}$), OMA-B-PEO ($0.3\text{--}3.87\text{ }\mu\text{mole ml}^{-1}$) and/or MA-B-PEO-F ($0.3\text{--}3.83\text{ }\mu\text{mole ml}^{-1}$) complex with HeLa and fibroblast cells at given molar concentrations for 24 h were stained by hematoxylen/eosin. The obtained results were illustrated in Fig. 7. The results of comparative morphological analyses indicated that a significant difference between HeLa cells and control group morphology does not observed at all used concentrations for 24 h (Fig. 7A-7C). Cell morphology is changed at relativelt higher concentrations for 24 h, but remained unchanged at middle concentrations for 24 h. Cell morphology of OMA-B has been changed at the $2.68\text{ }\mu\text{mole ml}^{-1}$ concentration via vacuole formation in their cytoplasms and lysing the cell membranes. Moreover, some of the cells have been detached from the well. When the

OMA-PEO-B-F complex was targetted to cancer cells by folic acid, its toxicity was higher than that without folic acid (OMA-B).

Double Staining and Caspase-3 Immunostaining Results

Apoptotic indexes in HeLa and fibroblast cells were estimated to be of caspase-3 and double staining results. Obtained results were summarized in Table II. Our crucial observations can be interpreted as follows: (i) If the cells were treated by OMA-B oligomer at $2.68 \mu\text{mole ml}^{-1}$ concentration, the number of apoptotic cells was relatively high. While the HeLa cells were treated with OMA-B-PEO-F complex at $2.36 \mu\text{mole ml}^{-1}$ concentration for 24 h, number of apoptotic cells increased. (ii) As for the organoboron oligomer-folic acid complex at $2.36 \mu\text{mole ml}^{-1}$ concentration, the number of apoptotic cells was high as well. (iii) The results of light and fluorescence microscope investigation of the interaction of organoboron oligomers with HeLa cells were illustrated in Fig. 8. As seen from these images, caspase-3 immunostaining result demonstrate that the cytoplasms of apoptotic cells treated with complex were turned brown (Fig. 8B) whereas that non-apoptotic cells did not (Fig. 8A). (iv) Double staining results showed that the non-apoptotic cell nuclei are stained lifeless blue (stained with Hoechst dye 33342) and exhibited smoothed nuclear morphology (Fig. 8C), but the apo-

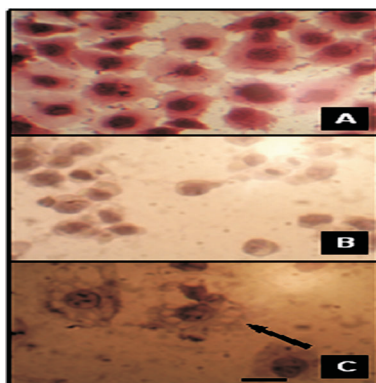


FIG. 7

Light microscope image of A non stained HeLa cell culture as a control, and B OMA-B-2-PEO oligomer ($650 \mu\text{g ml}^{-1}$)/HeLa cells conjugate (stained with hematoxilin-eosin dye); dense spots were showed nucleus of cells, and distinct violet were indicated cytoplasm of cells. Light microscope image of C vacuole of OMA-B oligomers ($650 \mu\text{g ml}^{-1}$)/HeLa cells cytoplasm; dense spots were showed nucleus of cells. All images were recorded under $\times 400$ magnification. Scale bar is $20 \mu\text{m}$

TABLE II

The comparative analysis of apoptotic and necrotic HeLa cells index for (I) oligo(maleic acid) (OMA) and its (II) organoboron amide (OMA-B-2), (III) poly(ethylene oxide)-branched (OMA-B-PEO) and (IV) folic acid-grafted (OMA-B-PFO-F) derivatives at 24 h incubation. Results are presented as means \pm SEM

(I)	[Oligomer], μ mole ml^{-1}				Apoptotic indexes, %				Necrotic indexes, %			
	(II)	(III)	(IV)	(I)	(II)	(III)	(IV)	(I)	(II)	(III)	(IV)	
0	0	0	0	0	2 \pm 1	1 \pm 1	1 \pm 1	1 \pm 1	1 \pm 1	1 \pm 1	1 \pm 1	
1.02	0.67	0.60	0.59	100	7 \pm 1	16 \pm 3	11 \pm 2	15 \pm 1	6 \pm 2	10 \pm 1	2 \pm 1	
2.04	1.34	1.20	1.18	200	12 \pm 2	20 \pm 2	18 \pm 3	25 \pm 3	20 \pm 3	35 \pm 3	15 \pm 1	
4.08	2.68	2.40	2.36	400	17 \pm 4	26 \pm 3	22 \pm 2	29 \pm 2	31 \pm 2	48 \pm 4	25 \pm 3	
6.63	4.36	3.87	3.83	650	14 \pm 1	12 \pm 2	14 \pm 1	15 \pm 1	38 \pm 3	65 \pm 5	41 \pm 2	
												49 \pm 5

ptotic cell nuclei stained bright blue and are compartmentalized (Fig. 8D). (v) The number of apoptotic cells decreased when the HeLa cells are treated with PEO-containing oligomers. However, the number of apoptotic cells was increased while having been treated with OMA-PEO-B-F complex targeted by folic acid at $2.36 \mu\text{m ml}^{-1}$ concentration in HeLa cells culture for 24 h. (vi) The double staining and caspase-3 immunostaining results show similarities with each other in HeLa cells. (vii) The obtained apoptotic indexes of Fibroblast cells were changed as per the studied functional oligomer system as follows: OMA (11%), OMA-B (17%), OMA-PEO-B (19%) and OMA-PEO-B-F (21%) at 4.08, 2.68, 2.4 and $2.36 \mu\text{m ml}^{-1}$ concentrations, respectively. Moreover, any significant change was not observed in apoptotic index of fibroblast cells while having been targeted by folic acid. As a result, folic acid targeted complex (OMA-PEO-B-F) was more apoptotic than OMA and its derivatives at chosen micromolar concentrations for 24 h in HeLa cells culture. Necrotic effect of OMA and its derivatives was determined using double staining method (cells nuclei stained with PI dye). Obtained

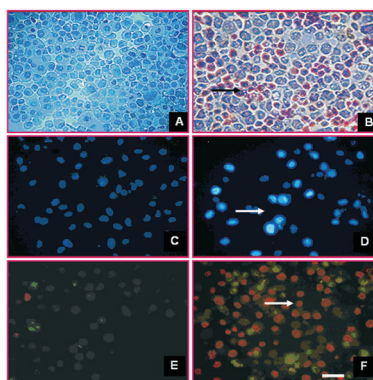


FIG. 8

Light microscope images of A virgin (non-apoptotic) HeLa cells as a control group (stained with caspase-3 immunostaining kit), and B OMA-B oligomer ($400 \mu\text{g ml}^{-1}$)/HeLa cells conjugate (stained with caspase-3 immunostaining kit), where brown cytoplasm of cells image indicates the formation of apoptotic cells. C Fluorescent microscope image of nucleus of untreated HeLa cells as a control, where formation of lifeless spots demonstrates nucleus of non-apoptotic cells. D Nucleus of HeLa cells (stained with Hoechst 33342), where bright spots indicate nucleus of apoptotic cells. E Fluorescent microscope image of nucleus of untreated HeLa cells as a control, where formation of green spots demonstrates nucleus of non-necrotic cells. F Nucleus of HeLa cells (stained with PI dye), where red spots indicate nucleus of necrotic cells and green spots indicate nucleus of non-necrotic cells (stained with Hoechst 33342). All images were recorded with $\times 400$ magnification. Scale bar is $20 \mu\text{m}$

results were presented in Table II. The OMA-B oligomers with lower concentrations (0.33–1.34 $\mu\text{mol ml}^{-1}$) are poor in necrosis stained with PI dye. The number of necrotic cells increases especially as they are treated with OMA-B at higher concentrations (2.68 $\mu\text{mole ml}^{-1}$ and above) in HeLa cells culture (Table II and Fig. 8F). However, when the cancer cells were treated with OMA-B-PEO, the necrotic indexes decreased in HeLa and fibroblast cells. Fluorescent microscope image of nucleus of untreated HeLa cells as control cells were presented in Fig. 8E, in which formation of green spots displays the nucleus of non-necrotic cells. If the HeLa cells are treated with oligomer targeted by folic acid (OMA-B-PEO-F), number of necrotic cells (necrotic cell nuclei is stained red by PI) yield high value (Fig. 8F). HeLa and fibroblast cells treated with oligomer and its functional derivatives lyse the cell membrane (necrosis). The obtained necrotic indexes of fibroblast cells were changed as per the studied organoboron oligomer system as follows: OMA (32%), OMA-B (51%), OMA-PEO-B (37%), and OMA-PEO-B-F (48%). It is worthy to note that incubation of HeLa and fibroblast cells for 24 h at higher micromolar concentrations of oligomer and its derivatives produces necrosis supporting its high toxic effect. As a result, folic acid targeted complex was not more necrotic toward HeLa cells than fibroblast cells. We have determined the more necrotic effect of OMA-B-PEO-F complex toward HeLa cells than fibroblast cells at 3.83 $\mu\text{mole ml}^{-1}$ concentration for 24 h.

CONCLUSIONS

This work presents the synthesis and characterization of organoboron, PEO branched and folic acid complexed derivatives of maleic anhydride oligomer and investigation of their antitumor activity (cytotoxicity, apoptotic and necrotic effects) toward HeLa and fibroblast cells by using a combination of various biochemical, statistical and microscopy methods. It was observed that antitumor activity significantly depends on the structure, amount of ionizable free carboxylic groups, organoboron linkages and complexed fragments in the functionalized oligomers, and changes in the following row: OMA << (OMA-B)s < OMA-B-PEO-FA. Apoptotic indexes in cancer and normal cells were estimated of caspase-3 immunostaining and double staining (Hoechst 33342 and PI) results. These observations are confirmed the realization of apoptosis and necrosis processes in the interaction of functionalized oligomers with HeLa cells than fibroblast cells. HeLa and fibroblast cells incorporated with OMA-B oligomer provide a lysing the cell membrane (necrosis) and relatively higher necrotic indexes 65 and 51% for the cancer and normal cells, respectively. It was found that interactions of

both the cells with OMA-B-PEO-F complexes were decreased the necrotic indexes for HeLa (49%) and fibroblast cells (45%). Thus, the results of these studies allow us to utilize the synthesized organoboron oligomers and their PEO branched and FA complexed derivatives in boron-neutron capture therapy (BNCT), which will be a subject of our furture investigations.

Supports: TAEK and TÜBITAK (Turkish National Scientific and Technology Research Council) – TBAG-2386 project.

REFERENCES

1. Gaylord N.: *Polym. Rev.* **1975**, *13*, 235.
2. Trivedi B. C., Culbertson B. M.: *Maleic Anhydride*. Plenum Press, New York 1982.
3. Rzaev Z. M. O.: *Polymers and Copolymers of Maleic Anhydride* (Russ.). Elm, Baku 1984; *Chem. Abstr.* **1985**, *102*, 114108w.
4. Bhadani S. N., Saha U. S.: *Makromol. Chem., Rapid Commun.* **1980**, *1*, 91.
5. Ryan M. E., Hynes A. M., Badyal J. P. S.: *Chem. Mater.* **1996**, *8*, 37.
6. Tomescu M., Macarie L.: *Mater. Plast.* **1975**, *12*, 25.
7. Braun D., Sayedl A. A., Pamakis J.: *Makromol. Chem.* **1969**, *124*, 249.
8. Hamann S. D.: *J. Polym. Sci., Part A* **1967**, *5*, 2939.
9. Holmes-Walker W. A., Weale K. E.: *J. Chem. Soc.* **1955**, *77*, 2295.
10. Babare L. V., Dremin A. N., Mikhailova A. N., Yakovlev V. V.: *Vysokomol. Soedin., Ser. B* **1967**, *9*, 642.
11. Charles M.-H., Delair T., Jaubert M., Mandrand B. F.: U.S. 5,489,653 (1996).
12. Solomon B., Levin Y.: *Biotechnol. Bioeng.* **1974**, *16*, 1161.
13. Petasis N. A.: *Aust. J. Chem.* **2007**, *60*, 795.
14. Yang W., Gao X., Wang B.: *Med. Res. Rev.* **2003**, *23*, 346.
15. Rzayev Z. M. O., Beşkardeş O.: *Collect. Czech. Chem. Commun.* **2007**, *72*, 1591.
16. Kahraman G., Beşkardeş O., Rzaev Z. M. O., Pişkin E.: *Polymer* **2004**, *45*, 5813.
17. Rzayev Z. M. O., Erdogan D., Türk M., Pişkin E.: *J. Biol. Chem. (Hacettepe University)* **2008**, *36*, 83.
18. Morin C.: *Tetrahedron* **1994**, *50*, 12521.
19. Baldock C., Boer G.-J. D., Rafferty J. B., Stuitje A. R., Rice D. W.: *Biochem. Pharmacol.* **1998**, *55*, 1541.
20. Jabbour A., Steinberg D., Dembitsky V. M., Moussaieff A., Zaks B., Srebnik M.: *J. Med. Chem.* **2004**, *47*, 2409.
21. Benkovic S. J., Baker S. J., Alley M. R. K., Woo Y. H., Zhang Y. K., Akama T., Mao W., Baboval J., Ravi Rajagopalan P. T., Wall M., Kahng L. S., Tavassoli A., Shapiro L.: *J. Med. Chem.* **2005**, *48*, 7468.
22. Baker S. J., Zhang Y. K., Akama T., Lau A., Zhou H., Hernandez V., Mao W., Alley M. R. K., Sanders V., Plattner J. J.: *J. Med. Chem.* **2006**, *49*, 4447.
23. Zhou H.-B., Nettles K. W., Bruning J. B., Kim Y., Joachimiak A., Sharma S., Carlson K. E., Stossi F., Katzenellenbogen B., Greene G.: *Chem. Biol.* **2007**, *14*, 659.
24. Valliant J. F., Guenther K. J., King A. S., Morel P., Schaffer P., Sogbein O. O., Stephenson K. A.: *Coord. Chem. Rev.* **2002**, *232*, 173.

25. Chen W., Mehta S. C., Lu D. R.: *Adv. Drug Deliv. Rev.* **1997**, *26*, 231.
26. Vazquez C. M., Navarro S. (Eds): *New Approaches in the Treatment of Cancer*. Nova Science Publishers, New York 2010.
27. Türk M., Rzayev Z. M. O., Kurucu G.: *Health* **2010**, *2*, 53.
28. Ulukaya E., Kurt A., Wood E. J.: *Cancer Invest.* **2001**, *19*, 145.
29. McPartland J. L., Guzail M. A., Kendall C. H., Pringle J. H.: *Int. J. Exp. Pathol.* **2005**, *86*, 19.
30. Bressenot A., Marchal S., Bezdetnaya L., Garrier J., Guillemin F., Plénat F.: *J. Heterocycl. Chem.* **2009**, *57*, 289.
31. Nobumichi O., Shintaro S.: *J. Macromol. Sci., Pure Appl. Chem.* **1990**, *7*, 861.
32. Schosselet F., Ilmain F., Candau S. J.: *Macromolecules* **1991**, *24*, 225.
33. Shimizu T., Minakata A.: *Eur. Polym. J.* **2002**, *38*, 1113.